JPE 9-3-12

ICPE'07 Selected Paper

Improved Flux and Torque Estimators of a Direct Torque Controlled Interior PM Machine with Compensations for Dead-time Effects and Forward Voltage Drops

Saad Sayeef † and M. F. Rahman*

†*School of Electrical Engineering and Telecommunications, University of New South Wales, Sydney, Australia

ABSTRACT

The performance of direct torque controlled (DTC) interior permanent magnet (IPM) machines is poor at low speeds due to a few reasons, namely limited accuracy of stator voltage acquisition and the presence of offset and drift components in the acquired signals. Due to factors such as forward voltage drop across switching devices in the three phase inverter and dead-time of the devices, the voltage across the machine terminals differ from the reference voltage vector used to estimate stator flux and electromagnetic torque. This can lead to instability of the IPM drive during low speed operation. Compensation schemes for forward voltage drops and dead-time are proposed and implemented in real-time control, resulting in improved performance of the space vector modulated DTC IPM drive, especially at low speeds. No additional hardware is required for these compensators.

Keywords: Permanent magnet synchronous motor, Direct torque control, Dead-time, Forward voltage drop

1. Introduction

Direct torque control (DTC) of Interior Permanent Magnet Synchronous Machines (IPMSM) was proposed and developed in the late 1990's[1-4]. DTC have also been implemented on reluctance synchronous and induction machines[5,6]. Some of the advantages of DTC over the conventional Field Oriented Control (FOC) include fast torque and stator flux dynamics, less machine parameter dependence, the elimination of the dq-axis current controllers, associated coordinate transformation, the rotor position sensor requirement and separate voltage pulse width modulator.

However, a major drawback of DTC is its poor performance at low speed which researchers have not been able to solve. The poor performance at low speed is due to a few reasons, namely limited accuracy of stator voltage acquisition and the presence of offset and drift components in the acquired signals.

In this paper, the effect of forward voltage drop and dead-time of power devices on a space vector modulation (SVM) integrated direct torque controlled IPMSM drive system is investigated. It is found that the voltage drop across power switches and power diodes is not negligible for flux and torque estimation at low speeds. The effect of forward voltage drop and dead-time becomes more significant for flux estimation when the machine operates

Manuscript received January 31, 2009; revised March 22, 2009.
†Corresponding Author: z3125688@student.unsw.edu.au
Tel:+61293855904 , Fax: +93855993, Univ. of New South Wales
*School of Electrical Engineering and Telecommunications, University of New South Wales, Sydney, Australia

at low speeds as it becomes comparable to the low applied voltage on the machine terminals. Holtz and Quan have examined and compensated for the effect of forward voltage drop on a vector controlled induction motor drive [7]. In this paper, a compensation method using additional voltage vectors is used and experiments were carried out to test the compensation scheme. Experimental results show that a better low-speed flux control has been achieved with the integration of the compensation schemes.

This paper is organized as follows. A brief background of a direct torque controlled IPM synchronous motor drive is given in Section 2. The effects of forward voltage drop and dead-time of switching devices in the inverter are discussed in Section 3. Experimental results to show the effects on flux and torque estimation error are presented in Section 4. The proposed compensation algorithm for improved flux and torque estimation is described in Section 5 and its effectiveness on the performance of the DTC IPM drive is investigated with experimental results in Section 6. Some conclusions are given in Section 7.

2. Direct Torque Control of an IPMSM

The basic principle of DTC is to select stator voltage vectors directly according to the differences between the reference and actual torque and stator flux linkage. The current controller followed by a pulse width modulation (PWM) comparator used in vector control is not required in DTC systems, and the parameters of the motor are also not used, except for the stator resistance. Therefore, DTC has the advantages of lesser parameter dependence and fast torque response when compared with the torque control via PWM current control [8].

Fig. 1 shows the system diagram of a DTC IPM drive integrated with space vector modulation (SVM), which will be referred to as PI-DTC drive in this paper. It includes flux and torque estimators, a Proportional + Integral (PI) torque controller, reference flux vector calculator and a space vector modulation block. A DC bus voltage sensor and two output current sensors are needed for the flux and torque estimation. Speed sensor is not necessary for the torque and flux control.

The PI torque controller outputs the reference angular frequency of the stator flux linkage from the difference between the actual and reference torque commands at its input. The reference flux vector is then calculated using the reference angular frequency, position of the estimated stator flux linkage and amplitude of the reference flux linkage, as shown in Fig. 2 [8]. The voltage space vectors and their duration are then selected and calculated according to the error flux linkage vector to reduce the error to zero.

In order to estimate the stator flux, λ, and torque, T, an integrator is used in (1), of which the scalar form is (2). The voltage vector, v, can be obtained by multiplying the DC bus voltage with the selected voltage space vector and the current vector can be obtained by measuring any 2 of the 3 phase currents. The torque is estimated by (3).

$$\lambda = \int (v - Ri)dt + \lambda_0 \tag{1}$$

$$\begin{aligned} \lambda_\alpha &= \int (v_\alpha - Ri_\alpha)dt + \lambda_{\alpha 0} \\ \lambda_\beta &= \int (v_\beta - Ri_\beta)dt + \lambda_{\beta 0} \end{aligned} \tag{2}$$

$$T = \frac{3}{2} p(\lambda \times i) = \frac{3}{2} p(\lambda_\alpha i_\beta - \lambda_\beta i_\alpha) \tag{3}$$

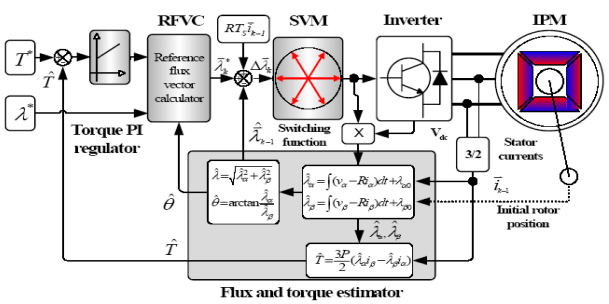

Fig. 1. System diagram of the PI DTC drive.

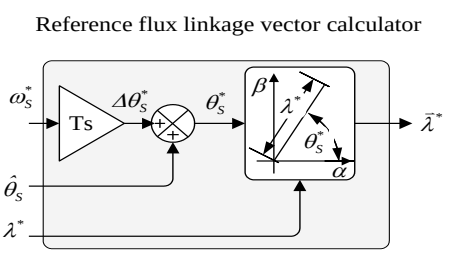

Fig. 2. Signal flowchart of the RFVC block.

where R is stator resistance, I the stator current, p the number of pole pairs, and the subscripts α, β, and 0 represent the α-β stationary reference frame components and initial state respectively.

It is seen from (1), (2) and (3) that the key for a good performing DTC is flux estimation. If the estimated flux drifts from the actual value of the flux linkage, the estimated torque will be wrong. In order to estimate the flux linkage accurately, accurate values for voltage vector, stator resistance, and initial rotor flux linkage and current vector must be known.

In the space vector modulated (SVM) DTC drive, the reference stator voltage vector V_{ref} is used for the estimation of stator flux, instead of the actual stator voltage vector seen at the machine terminal, to eliminate errors and offsets caused by sensing hardware and electric isolation. Sensing voltage vectors from the machine terminals has the problem of high harmonics which would require large filters and hence would introduce unacceptable delay. The V_{ref} signal is readily available in the Proportional + Integral (PI) direct torque controller and is free from harmonic components. However, it does not exactly represent the voltage vector at the machine terminals due to the distortions introduced by the dead-time and forward voltage drops inside the inverter [7]. The compensation must be made to the reference voltage vector which is used by the observers or estimators as an input for stator flux estimation.

At low speeds, the back EMFs are too small to be used to obtain accurate stator flux estimation. The stator flux estimation using pure integrator or a programmable low pass filter is still needed for start-up and very low speed operation close to zero. DC offset compensation is an important factor in a practical implementation of the integration since drift can cause large errors of the amplitude and position of the stator flux linkage space vector, which may make the drive system unstable in the very low speed region.

3. Non-linear Inverter Model

A three-phase two level IGBT inverter similar to that shown in Fig. 3 would normally be used for a three phase IPM motor. Voltage drops across the power switches in the inverter reduce the terminal voltage seen by the machine. At very low speeds, the voltage drop can be higher than the induced voltage and hence introduce severe disturbance.

According to the forward characteristic of the power devices illustrated in Fig. 4, the forward voltage drop across the IGBT and diode (v_{CE}) can be modelled by an average threshold voltage v_{CE0} and a current-dependent $r_{CE}i$, where r_{CE} is the differential resistance and i is the forward current of the device. This characteristic is expressed in (4) and represented by the dotted line in Fig. 4.

$$v_{CE} = v_{CE0} + r_{CE} \bullet i \tag{4}$$

It is well known that forward characteristics of the IGBT and its freewheeling diode are non-linear, as illustrated in Fig. 4. The focus in this paper is to compensate for the error caused by v_{CE0}.

It is well known that forward characteristics of the IGBT and its freewheeling diode are non-linear, as

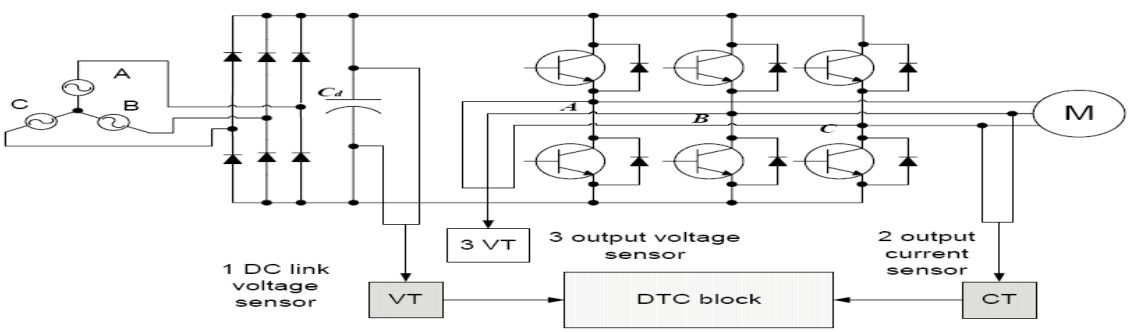

Fig. 3. Circuit diagram of the three phase two level inverter with a DTC Controller.

illustrated in Fig. 4. The focus in this paper is to compensate the error caused by v_{CE0}.

In order to examine the error in the voltage vector caused by neglecting the forward voltage drop, the switching modes of the inverter with different voltage vector and polarity are investigated. The operation mode of one inverter leg is analyzed in Fig. 5. The letter *s* in Fig. 5 indicates the switching function of the inverter leg. Output voltage of the inverter leg with positive current (into the load) and negative current (from the load) are compared under the conditions of *s=1* and *s=0*. It is seen that when the current is positive, the actual voltage is shifted down by v_{CE} and when the current is negative, the waveform of the actual output voltage is shifted up by v_{CE}. As a result, the error caused by the forward voltage drop of the switches of the inverter leg A can be expressed as in (5). The error voltage vector of the three inverter legs can be represented by (6).

$$\Delta v_A = s * v_{DC} - v_A = v_{CE0} * sgn(i_A) \tag{5}$$

$$V_{fvd} = \frac{2}{3} v_{CE}[\text{sgn}(i_A) + \alpha * \text{sgn}(i_B) + \alpha^2 * \text{sgn}(i_C)] \tag{6}$$

where $\alpha = e^{j2\pi/3}$, v_A is the voltage across inverter leg A, v_{DC} is the inverter input DC voltage and V_{fvd} is the forward voltage drop of the inverter.

From (6), it is seen that the voltage error vector only depends on the polarity of the three-phase currents and the switching status does not affect the error vector. Hence, for the purpose of compensating the error vector, only the polarities of the three phase currents are needed.

There is a time in each switching cycle where both the high and low side switches in the same leg of the inverter are off and the current flow is through diodes. This is known as the dead-time which is inserted into the gate signal of the switch that is to be turned on to avoid direct short circuit across the DC bus voltage source. This dead-time delay causes a change in and distortion of the stator voltage vector applied to the machine [9-11].

Fig. 6 shows the PWM control signal as an example and the switching signals of a single inverter leg. The control signals for the upper and lower switches are shown together with the dead-time. The turn-on and turn-off time of the power switches are also considered in the figure. In the last two subplots of Fig. 6, the expected and the actual output voltages are compared. It is seen that due to the effect of dead-time t_d, the turn-on delay t_{ON} and the turn-off delay t_{OFF}, there is distortion between the expected and the actual output voltages.

The dead-time error vector between the expected output and actual voltage vector is given by (7) for different directions of the current vector. This error can be compensated by detecting the polarity of the output current.

$$V_{dt} = \frac{2}{3} v_{dead}[\text{sgn}(i_A) + \alpha * \text{sgn}(i_B) + \alpha^2 * \text{sgn}(i_C)] \tag{7}$$

$$V_{dead} = \left(\frac{t_{dead} + t_{on} - t_{off}}{T_s} \right) \left(V_{dc} + V_{diode} - V_{sat} \right) \tag{8}$$

where $t_{dead}, t_{on}, t_{off}, V_{sat}, V_{dc}$ and T_s are dead time, turn-on time, turn-off time, average on-state voltage, dc-link voltage and switching period respectively.

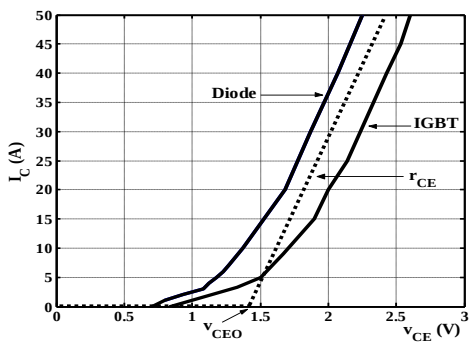

Fig. 4. Forward characteristics of the IGBT and diode in the three phase inverter.

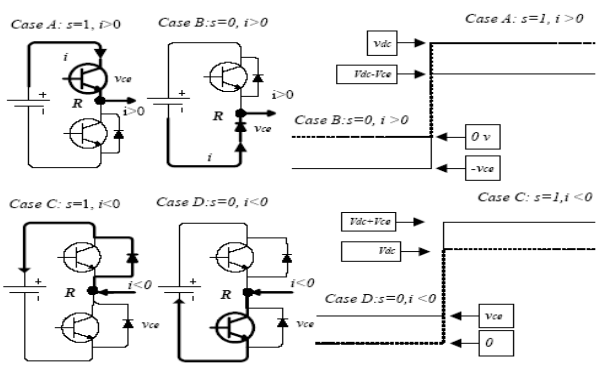

Fig. 5. Analysis of forward voltage drop of an inverter leg.

4. Experiment results without compensation

Experiments were performed to investigate the accuracy of flux and torque estimation at various speeds without any compensation for non-linear effects of the inverter. A DS1104 DSP card is used to carry out the real-time algorithm. A three-phase insulated gate bipolar transistor (IGBT) intelligent power-module is used for an inverter. Coding of real time control software was done using C language. The experimental setup is shown in Fig. 7. Space vector PWM signals were generated on the DS1104 board. An incremental encoder is used to detect the rotor speed and a DC machine is used to load the PM machine. Table 1 shows the parameters of the IPM motor used.

Table 1 Parameters of the IPM motor used

Number of pole pairs	P	2
Rated power	P_r	1 kW
Phase Voltage	V	132V
Stator resistance	R	5.8 Ω
Magnet flux linkage	λ_f	0.533 Wb
d-axis inductance	L_d	0.0448 H
q-axis inductance	L_q	0.1024 H
Phase current	I	3 A
Base speed	w_b	1260 rpm
Rated torque	T_b	6 Nm

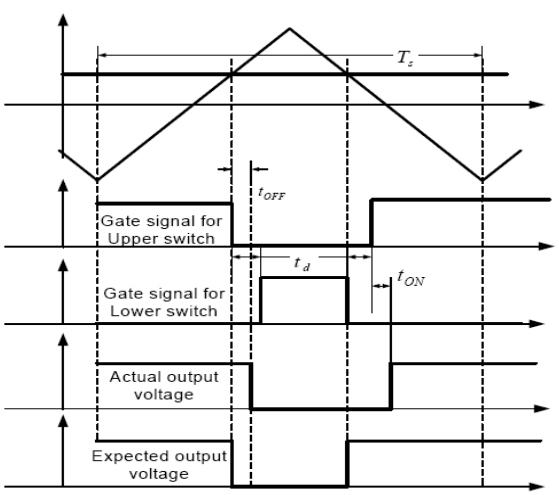

Fig. 6. PWM switching signals of the inverter with positive current considering the effect of dead-time and switc hing delays in the power switches.

Fig. 11 shows the dynamic response of the PI-DTC IPM drive during speed transition from 200 rpm to 800 rpm. The flux and torque estimation errors are seen to be larger at 200 rpm than at the higher speed of 800 rpm, indicating the necessity for compensation at low speed.

The performance of the PI-DTC IPM drive at 500rpm with rated load without any compensation for non-linear effects of the inverter is shown in Fig. 8. It is seen that the estimated values of torque and flux are close to the actual values. Ideally, the estimated and actual values should exactly match each other. The performance at 186rpm is shown in Fig. 9. A significant deviation of the estimated torque and stator flux from the actual ones is observed, indicating a significant increase in estimation error at lower speed. Fig. 10 shows the corresponding speed, phase current and reference voltage (V_α) responses. The phase current at 186 rpm is a distorted sinusoid, as seen in Fig. 10, due to the effects of forward voltage drop and dead-time of inverter switching devices. The lowest speed at which the PI-DTC IPM drive can run smoothly under full load conditions without FVD and dead-time compensation is 186rpm.

5. Compensation algorithm

The compensation in (9) must be made to the reference voltage vector, V_{ref}, which is used by the estimators as the input $V_{\alpha,\beta}$ for more accurate observation. In order for the machine to run at a very low speed smoothly, the fundamental reference voltage must be compensated for the inverter device forward voltage drops and the dead-time loss using the estimated value of ΔV.

$$V_{\alpha,\beta} = V_{ref} - (V_{fvd} + V_{dt}) = V_{ref} - \Delta V \tag{9}$$

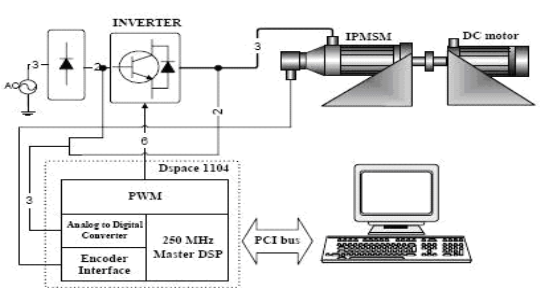

Fig. 7. Experimental setup used for IPM drive control.

Fig. 12 shows a block diagram of the process for compensating for the effects of forward voltage drop and dead-time of power devices in the three-phase inverter required for more accurate estimation of stator flux and torque. The inputs to the compensation logic block are the polarities of the three phase currents, forward voltage drop across the IGBT and diode v_{CE} shown in (4) and voltage drop due to dead-time, turn-off and turn-on delays v_{dead} shown in (8). The compensation logic block uses (6) and (7) to determine the error voltage vector, which is used to compensate the reference voltage vector for the purpose of flux and torque estimation.

From (6) and (7), it is noticed that the line to neutral voltage reduction in the stationary reference frame is a six-step waveform which is in phase with the corresponding phase current and has step values of $\frac{4}{3}\Delta V$, $\frac{2}{3}\Delta V$, $-(\frac{2}{3}\Delta V)$ and $-(\frac{4}{3}\Delta V)$. Fig. 13 illustrates the compensation voltage vectors and six sectors. Table 2 shows the compensation voltages as a function of phase current directions. For example, if the current vector is in region II as shown in Fig. 13, the error vector will be

$$\Delta v = -\frac{4}{3} v_{CEO} \alpha^2 \tag{10}$$

Table 2 Deadtime and forward voltage drop compensation voltages in sectors.

$sgn(i_A)$	$sgn(i_B)$	$sgn(i_C)$	Sector	$V_{\alpha,com}$	$V_{\beta,com}$
+	-	-	I	$\frac{4}{3}\Delta V$	0
+	+	-	II	$\frac{1}{2}\left(\frac{4}{3}\Delta V\right)$	$\frac{\sqrt{3}}{2}\left(\frac{4}{3}\Delta V\right)$
-	+	-	III	$-\frac{1}{2}\left(\frac{4}{3}\Delta V\right)$	$\frac{\sqrt{3}}{2}\left(\frac{4}{3}\Delta V\right)$
-	+	+	IV	$-\left(\frac{4}{3}\Delta V\right)$	0
-	-	+	V	$-\frac{1}{2}\left(\frac{4}{3}\Delta V\right)$	$-\frac{\sqrt{3}}{2}\left(\frac{4}{3}\Delta V\right)$
+	-	+	VI	$\frac{1}{2}\left(\frac{4}{3}\Delta V\right)$	$-\frac{\sqrt{3}}{2}\left(\frac{4}{3}\Delta V\right)$

6. Experiment Results with Compensation

The compensation scheme proposed in the previous section was implemented experimentally to investigate its effectiveness on the DTC IPM drive, especially at low speed. The compensation schemes are software oriented and no additional hardware is required. It should be noted that the problems of FVD and dead-time cannot be isolated in the real hardware of the inverter. The values of dead-time, turn-on and turn-off delay used in the compensation scheme are 3.5μs, 1μs and 1.5μs respectively. These parameters were obtained from the technical data sheet of the IGBT module PM50RHA120.

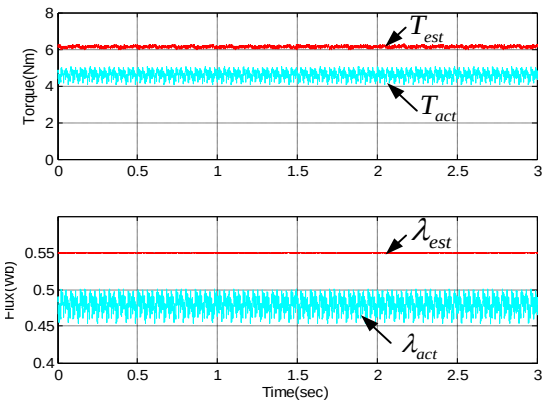

Fig. 8. Flux linkage and torque at 500rpm without compensation under full load condition.

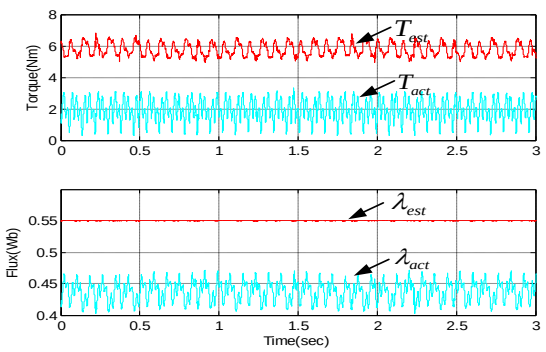

Fig. 9. Responses of torque and stator flux without FVD and dead-time compensation at 186rpm with full load.

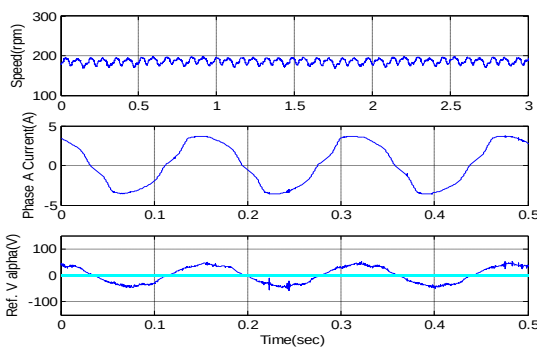

Fig. 10. Responses of rotor speed, phase current and reference voltage without FVD and dead-time compensation.

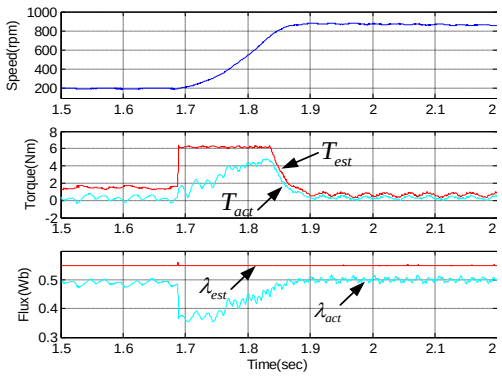

Fig. 11. Torque and flux linkage (actual and estimated) responses of PI-DTC during speed change from 200 rpm to 800 rpm without compensation.

A system diagram of the DTC IPM drive system with the integration of the compensation scheme is shown in Fig. 14. Two current sensors and one DC bus voltage sensor employed by the SVM DTC drive are still used.

Fig. 15 shows the estimated and actual flux linkages and torques of the PI-DTC IPM drive with compensations for forward voltage drop and dead-time at 500 rpm under full load condition. It can be seen that the estimated stator flux linkage and torque match the actual values well, indicating better performance than that seen in Fig. 8 without compensation. The estimated and actual stator flux linkages and torques at 186 rpm under full load condition is shown in Fig. 16. The estimated and actual values of torque and flux are not exactly the same but the difference between them is significantly smaller than that seen without compensation in Fig. 9. The phase current waveform at 186 rpm with compensation, in Fig. 17, is seen to be more sinusoidal than without compensation shown in Fig. 10. Hence, the compensation scheme effectively eliminates phase current distortions at low speeds. Fig. 18 shows the dynamic response of the compensated DTC IPM drive during speed step change from 150 rpm to 800 rpm. The estimated torques and stator flux linkages are seen to track their actual counterparts very well during the transition.

More accurate flux and torque estimation with the forward voltage drop and dead-time compensation integrated has enabled the PI-DTC IPM drive to operate down to 120 rpm with rated load and 60 rpm with half of the rated load. Therefore, better low speed performance of the PI-DTC IPM drive is achieved with the implementation of the proposed compensation algorithm for the effects of forward voltage drops and dead-time.

7. Conclusions

In this paper, the effects of the forward voltage drop and dead-time of power switches on the performance of space vector modulation integrated direct torque controlled IPMSM drive system are analysed and investigated. It is seen that the forward voltage drop and dead-time of power devices cause errors in the estimation of flux and torque, especially during very low speed operation, which could lead to instability and uncontrollability of the drive system.

A voltage vector based compensation scheme, which does not require any additional hardware, is proposed to improve the stator flux linkage and torque estimation of the drive. Experimental results show that a significantly better low speed performance of the PI-DTC IPM drive system is achieved with the implementation of the proposed compensation algorithm for the effects of forward voltage drop and dead-time.

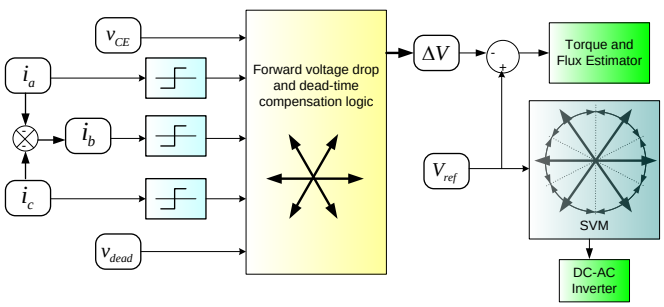

Fig. 12. Compensation for forward voltage drop and dead-time effects.

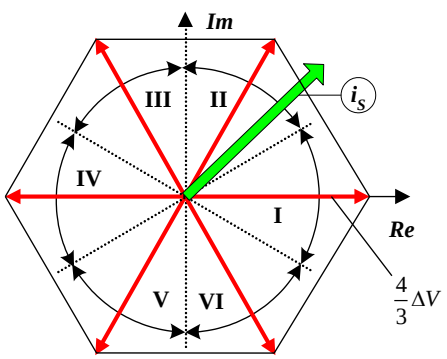

Fig. 13. Compensation voltage vectors and six sectors.

References

[1] L. Zhong, M.F. Rahman, Y Hu., "Analysis of direct torque co ntrol in permanent magnet synchronous motor drives," *Power Electronics, IEEE Transactions on*, Vol.12, No.3, pp. 528-53 6, 1997.

[2] C. French and P. Acarnley, "Direct torque control of perman ent magnet drives," *Industry Applications, IEEE Transaction s on*, Vol.32, No. 5, pp. 1080-1088, 1996.

[3] L. Zhong, M. F. Rahman, W. Y. Hu, and K. W. Lim, "A direct torque controlled interior permanent magnet synchronous motor drive incorporating field weakening," *IEEE Trans. Ind. Applicat.*,Vol.34, pp.1246-1253, Nov./Dec. 1998.

[4] M. F. Rahman, L. Zhong and K. W. Lim, "A direct torque controlled interior permanent magnet synchronous motor drive incorporating field weakening," *in Conf. Rec. IEEE-IAS Annu. Meeting*, Vol.1, pp. 67-74, 1997.

[5] H. Lee, H. Nguyen and T. Chun, "Implementation of Direct Torque Control Method using Matrix Converter Fed Induction Motor," *Journal of Power Electronics*, Vol. 8, No. 1, pp. 74-80, January 2008.

[6] M. Kim, "Direct Torque Control of a Reluctance Synchronous Motor Using a Neural Network," *Journal of Power Electronics*, Vol. 5, No. 1, pp. 36-44, 2005.

[7] J. Holtz, and Q. Juntao, "Drift- and parameter-compensated flux estimator for persistent zero-stator-frequency operation of sensorless-controlled induction motors," *Industry Applications, IEEE Transactions on*, Vol.39, No.4 pp. 1052-1060, 2003.

[8] L. Tang, L. Zhong, M.F. Rahman and Y. Hu, "A novel direct torque controlled interior permanent magnet synchronous machine drive with low ripple in flux and torque and fixed switching frequency," *Power Electronics, IEEE Transactions on*, Vo.19, No.2, pp. 346-354, 2004.

[9] Z. Xu, "Robust and Improved Flux Estimator and Controller Designs for Direct Torque Controlled Interior Permanent Magnet Synchronous Motors," PhD Thesis, Electrical Engineering and Telecommunication, The University of New South Wales, 2005.

[10] H. Kim, H. Moon and M. Youn, "A Novel Dead-Time Compensation Method using Disturbance Observer," *Journal of Power Electrinocs*, Vol. 2, No. 1, pp. 55-66, January 2002.

[11] N. Urasaki, T. Senjyu, T. Funabashi and H. Sekine,"An Adaptive Dead-time Compensation Strategy for a Permanent Magnet Synchronous Motor Drive Using Neural Network," *Journal of Power Electronics*, Vol. 6. No.4, pp.279-289, 2006.

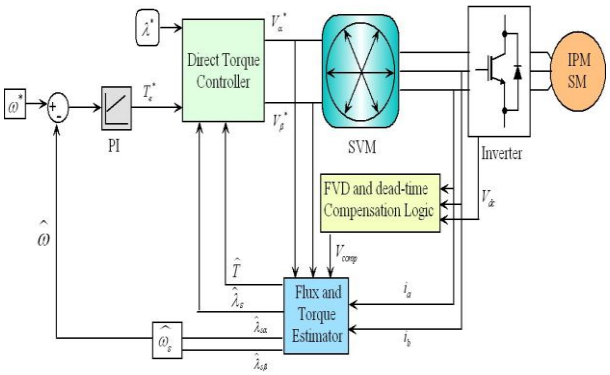

Fig. 14. Sensorless DTC IPM drive system with forward voltage drop and dead-time compensation.

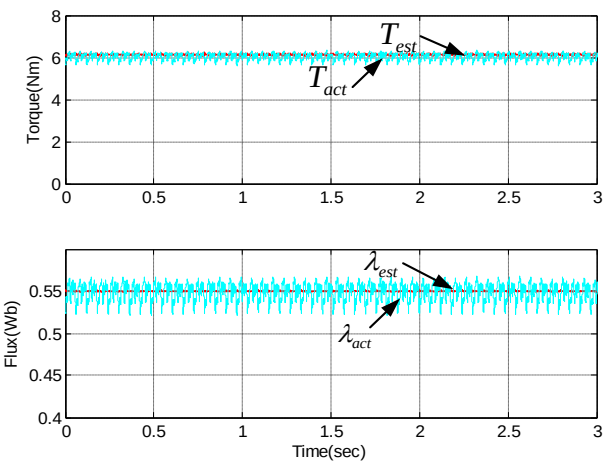

Fig. 15. Flux linkage, torque and current at 500rpm with FVD and dead-time compensation under full load condition.

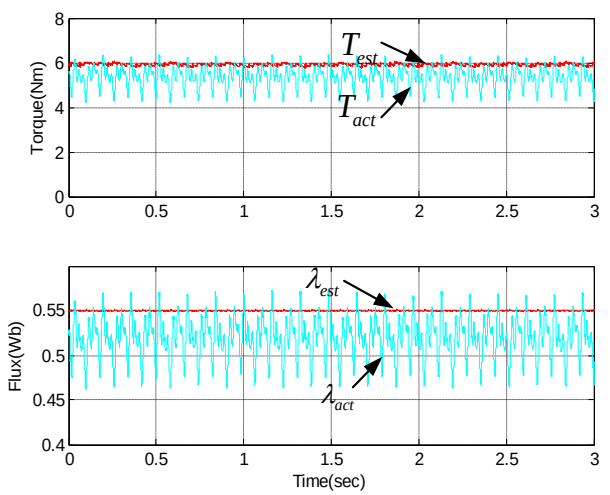

Fig. 16. Responses of torque and stator flux with FVD and dead-time compensation at 186rpm with full load.

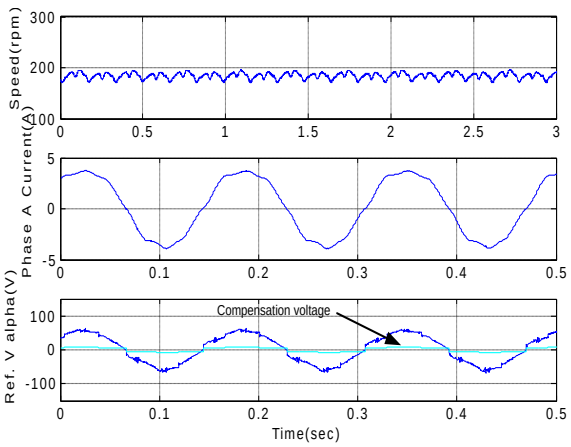

Fig. 17. Responses of rotor speed, phase current and reference voltage with FVD and dead-time compensation under full load.

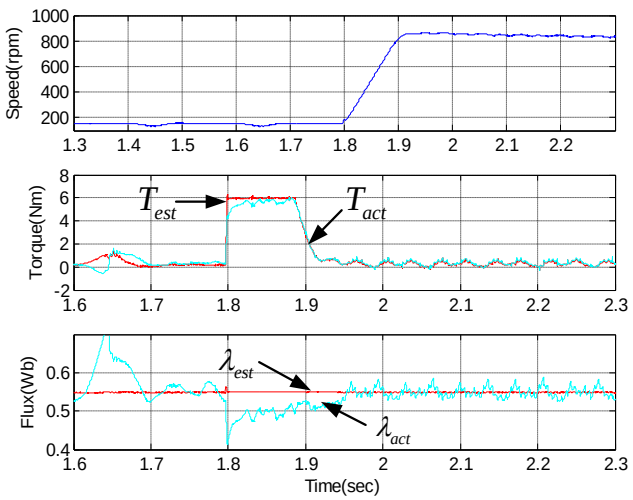

Fig. 18. Torque and flux linkage (actual and estimated) responses during speed change from 150 rpm to 800 rpm for PI-DTC drive with FVD and dead-time compensation.

Saad Sayeef received his Bachelor of Engineering (B. E.) degree in Electrical and Electronics Engineering with First Class Honours from the University of Auckland, New Zealand, in 2002. He was an Electronics Design Engineer at Fisher & Paykel Appliances Ltd in Auckland, New Zealand until 2004, and is currently in the process of completing his PhD degree at the University of New South Wales, Sydney, Australia. His research interests include power electronics, motor drive systems and renewable energy technologies.

M. F. Rahman (M'78-SM'94) majored in Electrical Engineering in 1972 from the Bangladesh University of Engineering and Technology. He obtained his Master and Ph.D. from the University of Manchester Institute of Science and Technology (UMIST), U. K., in 1975 and 1978, respectively. He subsequently worked as a systems design engineer at the General Electric Projects Co. of U. K. at Rugby, U/K., for two years before joining the National University of Singapore in 1980. He joined the University of New South Wales, Australia, in 1988 where he is now a full professor. His research interests are in electrical machines, power electronics, drives and associated control systems. He is a senior member of IEEE and is active in its Power Electronics, Industry Applications and Industrial Electronics societies.